SCIENTIFIC REPORTS

OPEN

SUBJECT AREAS:
METALLOPROTEINS
BIOCHEMISTRY
BIOINORGANIC CHEMISTRY
CANCER

Received
25 February 2013

Accepted
4 June 2013

Published
24 June 2013

Correspondence and requests for materials should be addressed to Z.-W.M. (cesmzw@mail.sysu.edu.cn)

V-Shaped Dinuclear Pt(II) Complexes: Selective Interaction with Human Telomeric G-quadruplex and Significant Inhibition towards Telomerase

Cui-Xia Xu[1], Yu-Xuan Zheng[1], Xiao-Hui Zheng[1], Qian Hu[2], Yong Zhao[2], Liang-Nian Ji[1] & Zong-Wan Mao[1]

[1]MOE Key Laboratory of Bioinorganic and Synthetic Chemistry, School of Chemistry and Chemical Engineering, Sun Yat-Sen University, Guangzhou 510275, China, [2]Key Laboratory of Gene Engineering of the Ministry of Education, State Key Laboratory of Biocontrol, School of Life Sciences, Sun Yat-Sen University, Guangzhou 510006, China.

A quaternized trigeminal ligand, 4-[4,6-di(4-pyridyl)-1,3,5-(2-triazinyl)]-1-methylpyridine-1-ium hexafluorophosphate (dptmp·PF_6), and two derivative V-shaped dinuclear Pt(II) complexes, {[Pt(dien)]$_2$(dptmp)}$(PF_6)_5$ (1) and {[Pt(dpa)]$_2$(dptmp)}$(PF_6)_5$ (2), were synthesized, characterized and applied to a series of biochemical studies. FRET and SPR analyses showed these compounds, especially Pt(II) complexes, bound more strongly to human telomeric (hTel) G-quadruplex than to promoters (such as c-myc and bcl2) or to the duplex DNA. PCR-stop assays revealed that the Pt(II) complexes could bind to and stabilize G-quadruplex far more effectively than corresponding ligand. CD analyses further indicated the three compounds likely stabilized the formation of mixed-type parallel/antiparallel G-quadruplex structures. Their efficacy as telomerase inhibitors and potential anticancer drugs was explored via TRAP. The IC_{50} value was determined to be 0.113 ± 0.019 μM for 1, indicating that it is one of the strongest known telomerase inhibitors. These results confirm that both V-shaped dinuclear Pt(II) complexes act as selective G-quadruplex binders and significant telomerase inhibitors.

In recent years, G-quadruplexes, which consist of four-stranded nucleic acids, and are described as presenting a high-order secondary DNA structure, have drawn attention regarding their potential use in anticancer therapies[1,2]. These guanine-rich sequences exist ubiquitously in significant regions of the eukaryotic genome, such as in the promoter regions of several oncogenes and the telomeres at the ends of the chromosomes[3–6]. It has been reported that telomerase is active and up-regulated in approximately 85% of tumor cells, which would lead to telomere elongation and contribute to cancer cell immortalization[7,8]. Thus, the telomeric G-quadruplex has been considered to be a potentially effective antitumor target[1,2]. The formation of a G-quadruplex would result in the inhibition of telomerase activity and would thereby terminate telomere maintenance[9]. Researches aimed at the stabilization of the G-quadruplex structure of certain sequences and efficiently inhibition of telomerase activity represent a rising field of research in anticancer drug design and development.

G-quadruplexes consist of stacked G-tetrads, which are formed from four guanine bases of G-rich sequences connected by Hoogsteen hydrogen bonds (Fig. 1a). Monovalent cations, such as potassium and sodium ions, can stabilize G-quadruplex structures, presumably via electrostatic interactions with the guanine carbonyl moieties. Previous studies addressing various G-quadruplex conformations have been reported, and crystallographic and NMR data have revealed that G-quadruplexes can be classified according to different strand orientations as showing a parallel structure[10] (Fig. 1b), mixed-type "(3 + 1) hybrid" structure[11] (Fig. 1c) or basket-type "(2 + 2) hybrid" structure[12] (Fig. 1d). These structural data provide important information for the development of G-quadruplex binders.

In past decades, many small molecules that interact with G-quadruplexes have been reported[13,14]. Some synthetic simple organic molecules[15–20], typically metal complexes[21–30], have been well characterized as effective G-quadruplex binders. Platinum(II) complexes, as successful inorganic anticancer drugs, have long been considered important due to their interaction with nucleic acids. Recently, planar platinum(II) complexes[24–30] have drawn increasing interests related to targeting telomeric G-quadruplex DNA. Some mononuclear platinum(II) complexes, including platinum(II)-phenanthroline[24,25], platinum(II)-terpyridine[26] and others, with positively

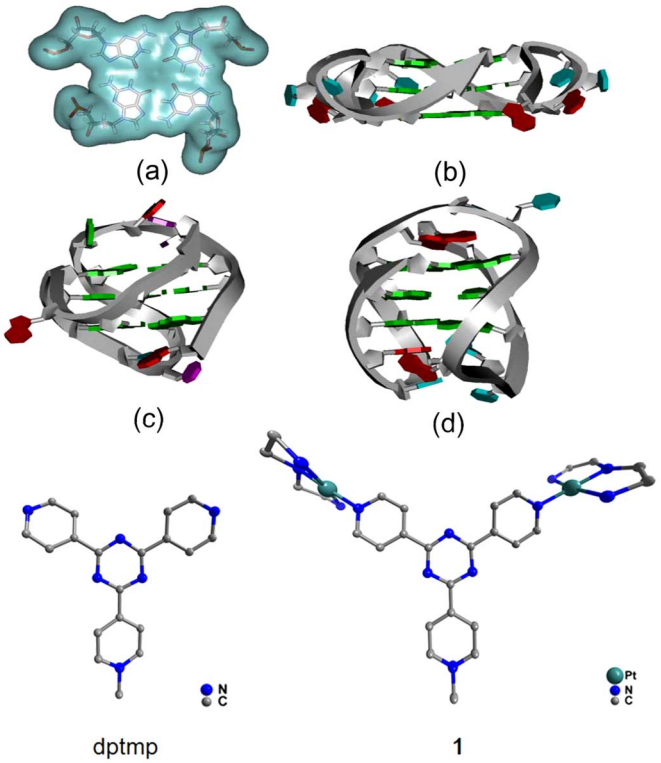

Figure 1 | Schematic representation of a G-tetrad and different conformations of G-quadruplexes; ORTEP views of dptmp and 1. (a) a G-tetrad consists of four guanines, (b) the wild-type 22-mer crystal with K^+ (parallel structure, PDB ID: 1KF1), (c) the modified 20-mer in K^+ solution (mixed-type "(3 + 1) hybrid" structure, PDB ID: 2KZD), (d) the wild-type 22-mer in Na^+ solution (basket-type "(2 + 2) hybrid" structure, PDB ID: 143D).

charged side arms, which interact readily with the negatively charged phosphate backbones, grooves and loops of the quadruplexes, have been reported. Additionally, a chain-like bidentate dinuclear platinum(II) complex[30] has been reported as a c-myc and hTel quadruplex binder. A kind of self-assembled tetranuclear platinum(II) complexes[27–29] with an aromatic plane was studied, which turned out to be good G-quadruplex binders, displaying evident telomerase inhibition. These studies have suggested that a large electron-deficient π-aromatic surface, positively charged area and positively charged substituents represent characteristics of a good G-quadruplex binder.

We have previously reported a series of mononuclear and tetranuclear Pt(II) complexes as G-quadruplex binders[28,29,31,32]. To further investigate the structure-activity relationship of various Pt(II) complexes, herein we synthesized a new bridged ligand by quaternizing a branch of a trigeminal star-like molecule, 4-[4,6-di(4-pyridyl)-1,3,5-(2-triazinyl)]-1-methylpyridine-1-ium iodide (dptmp·I) (CCDC 894005), and its derivative V-shaped dinuclear platinum(II) complexes, $\{[Pt(dien)]_2(dptmp)\}(PF_6)_5$ (**1**) (CCDC 894006) and $\{[Pt(dpa)]_2(dptmp)\}(PF_6)_5$ (**2**). Besides, the structures of dptmp and **1** have been successfully characterized by X-ray crystallography (shown in Fig. 1 and Supplementary Table S1).

Results

Synthesis of dptmp and Pt(II) Complexes $\{[Pt(L^x)]_2(dptmp)\}(PF_6)_5$. The compound dptmp·I was synthesized through the reaction of 2,4,6-tri(4-pyridyl)-1,3,5-triazine (tpt) with MeI. We tested several solvents (such as dichloromethane, trichloromethane, tetrachloromethane and N,N-dimethyl formamide) but could only obtain the pure product from trichloromethane. This was because dptmp·I precipitated from trichloromethane and could not undergo further substitution reactions. After heating the reaction mixture under reflux in trichloromethane for 48 h, it was filtered, the solvent was removed under reduced pressure and the residue was washed with trichloromethane. The isolated dptmp·I was characterized by ^1H and ^{13}C NMR spectroscopy, mass spectrometry and elemental analyses (see Experimental Details). Subsequently, dptmp·PF_6 was obtained through the reaction of dptmp·I with ammonium hexafluorophosphate.

The traditional method for synthesizing [Pt(dien)Cl]Cl·HCl involves the reaction of K_2PtCl_4 with diethylenetriamine (dien) dissolved in water (pH 3.0) by heating under reflux for 72 h followed by concentration until the yellow product precipitates out[33]. We employed a similar method, described by Annibale *et al.*[34], using $[Pt(COD)Cl_2]$[35] as an intermediate, which was found to be more convenient and resulted in a very high yield of 96.7%.

The complex $[Pt(L^x)Cl]Cl$ was first treated with $AgNO_3$ to eliminate the two chlorides, then filtered to remove AgCl and transferred to a stoppered flask, followed by the addition of dptmp·PF_6 and heated at 90°C for 72 h under N_2. Finally, excess ammonium hexafluorophosphate was added to the reaction mixture, and the obtained precipitate was filtered out. The two dinuclear Pt(II) complexes were fully characterized via ^1H, ^{13}C and ^{195}Pt NMR spectroscopy and elemental analyses. Additionally, dptmp·I and **1** were structurally characterized by X-ray crystallography (Fig. 1).

Selectively stabilize hTel G-quadruplex DNA structure. Fluorescence resonance energy transfer (FRET) studies were conducted to investigate the binding abilities of the three compounds to human telomeric, promoter G-quadruplex DNA sequences (hTel, c-myc and bcl2) and a duplex DNA sequence. Reliable FRET melting curves (Fig. 2) and stabilization temperature (ΔT_m) values (Table 1) were obtained[36]. As shown in Table 1, it was clear that the three compounds exhibited ΔT_m values >17°C with the human telomeric (hTel) G-quadruplex; in contrast, they presented ΔT_m values <6°C with c-myc, ΔT_m values <3°C with bcl2 and ΔT_m values <1.5°C with duplex DNA. At the same time, the two dinuclear Pt(II) complexes displayed high ΔT_m values with the hTel G-quadruplex of 35.4°C and 30.5°C at 0.5 μM, which were higher than that obtained for the quaternary ammonium ligand-dptmp (17°C at 0.5 μM).

To quantitatively investigate the binding constants between compounds and DNA samples (the hTel G-quadruplex and duplex DNA sequences), surface plasmon resonance (SPR) experiments were conducted (Supplementary Fig. S8 and Table 2), which serve as a powerful technique for monitoring molecular reactions in real time[37–43]. Figure S8 shows the SPR sensorgrams generated for the three compounds binding to the immobilized hTel G-quadruplex and duplex DNA at different concentrations. Based on the obtained data, shown in Table 2, the two Pt(II) complexes displayed higher binding constants with the hTel sequence compared to that with dptmp (dptmp, 4.00×10^5; **1**, 1.37×10^6 and **2**, 1.40×10^6). Regarding the binding selectivities between the hTel quadruplex and duplex sequences, **1** showed a higher selectivity of 7.1 fold (5,170 vs. 731 nM), compared to **2** at 4.7 fold (3,390 vs. 712 nM), while dptmp showed the lowest selectivity of 1.2 fold (2,890 vs. 2,500 nM). We also found that the kinetic binding affinities (K_A) of the three compounds with the hTel G-quadruplex were superior to those with the duplex DNA sequence.

Stabilizing hTel G-quadruplex structures. To further evaluate whether the compounds effectively bound to the tested oligomer HTG21 and stabilized the G-quadruplex structure, polymerase chain reaction (PCR) stop assays were performed[39–41]. In these assays, in the presence of the compounds, the template sequence can form a G-quadruplex structure, and PCR products of dsDNA will be undetectable.

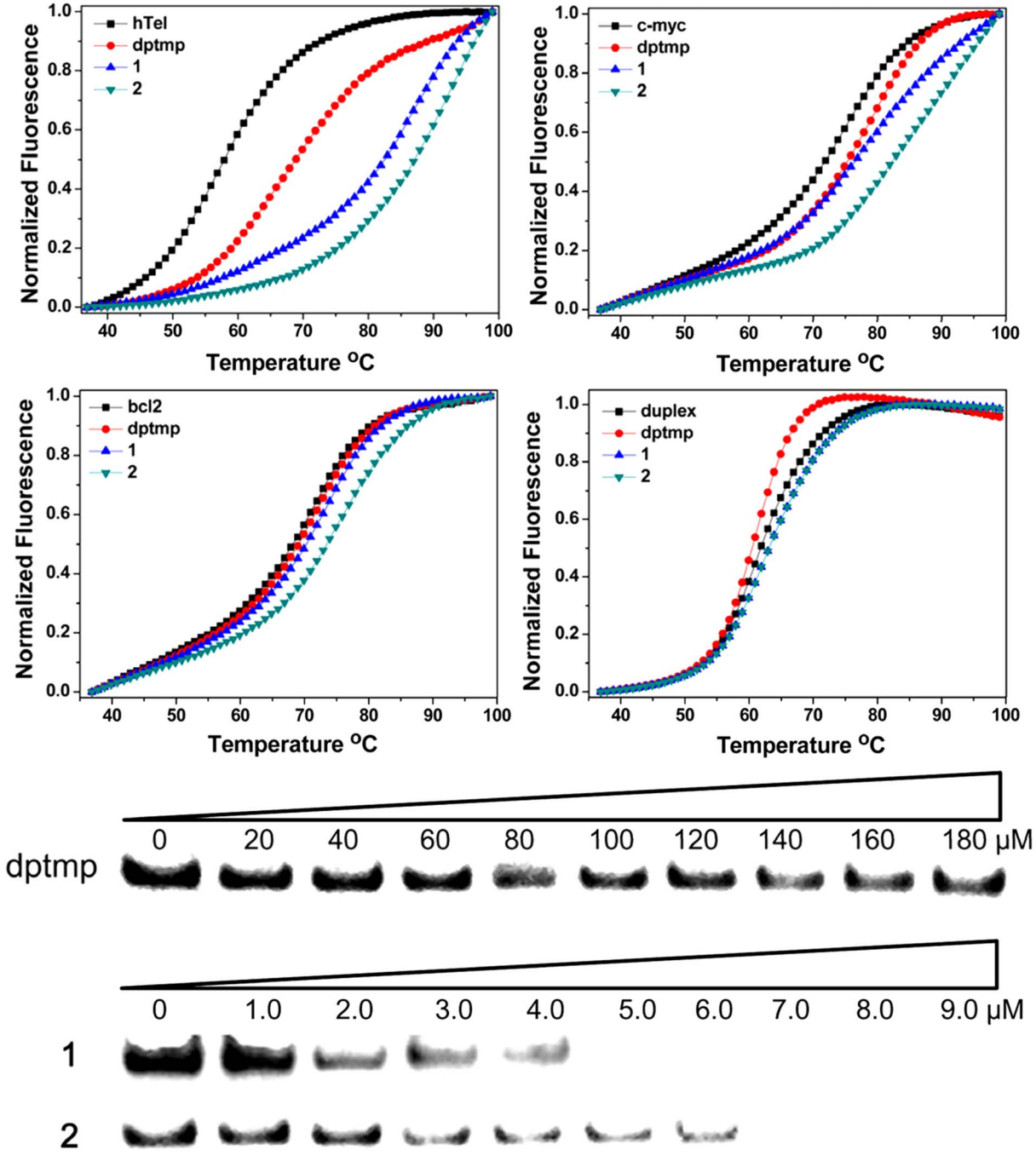

Figure 2 | Upper: FRET-melting curves[a] for experiments carried out with hTel, c-myc, bcl2 and duplex DNA separately with the three compounds (dptmp, 1 and 2). Lower: dose-dependent inhibition of PCR amplification by the different concentrations of the compounds (dptmp, 1 and 2) in the PCR-stop assays[b]. [a] All experiments were conducted at a DNA concentration of 400 nM and with a 0.5 μM concentration of the compounds, in Tris-HCl buffer (10 mM, pH 7.4) containing 60 mM potassium cacodylate buffer (DNA sequence: black; red: dptmp; blue: **1**, green: **2**). [b] The amplified PCR products were then analyzed on 15% non-denaturing polyacrylamide gels (100 V, 30 min) in 1× TBE buffer, followed by silver staining.

Figure 2 indicates that the inhibitory effects of complexes **1** and **2** were enhanced distinctly as the concentrations of both complexes increased from 1.0 to 9.0 μM, with no PCR products being detected at 5.0 or 7.0 μM, respectively. However, dptmp showed a weaker ability to inhibit the appearance of the PCR products and some PCR products were detected at 180 μM. The results indicated that the two complexes exhibited higher binding affinities for the G-quadruplex and were effective G-quadruplex binders. Moreover, to avoid any possible interaction of rTaq polymerase with the compounds and subsequent inhibition of the PCR process, we conducted parallel experiments using the mutated oligomer HIG21 mu instead of HIG21 under the same experimental conditions. The HIG21 mu sequence was unable to form a G-quadruplex. The obtained results suggested that the compounds could not significantly affect the activity of rTaq polymerase at comparable concentrations (Supplementary Fig. S10).

Induction of the formation of mixed-type parallel/antiparallel hTel G-quadruplexes and stabilization of this structure. Circular dichroism (CD) spectroscopy was performed to roughly characterize

Table 1 | Stabilization temperatures, ΔT_m (°C) for hTel, c-myc, bcl2 and duplex DNA stabilized by the three compounds determined from FRET[a]

	ΔT_m (°C)				
Compounds	hTel	c-myc	bcl2	duplex	C_{ML}/C_{DNA}
dptmp	17	4	0	0	1.25
1	35.4	3	0	0	1.25
2	30.5	6	3	1.5	1.25

[a]The concentration of hTel, c-myc, bcl2 and duplex DNA was 400 nM, with a 0.5 μM concentration of the compounds in 60 mM potassium cacodylate buffer (pH 7.4).

the structural conversion of various conformations of human telomeric G-quadruplexes, which consist of intra- and inter-molecular in parallel, antiparallel-stranded and mixed arrangements, depending on the strand orientations[37,44,45]. It has been reported that the CD spectra of the human telomeric DNA sequence (AG22) may consist of a mixed-type parallel/antiparallel G-quadruplex conformation in the presence of potassium cations, and usually show a strong positive peak around 290 nm, a small positive peak at 265 nm and a small negative peak at 240 nm[46–48]. On the other hand, in the presence of sodium cations, the CD spectra consist of a positive band near 295 nm and a negative band at 265 nm, which may be characteristics of a typical antiparallel G-quadruplex structure[12,49]. In the absence of metal ions, the CD spectra of the AG22 sequence indicate the coexistence of single strand, parallel and antiparallel G-quadruplexes[31,37,38,44–47].

In the current studies, the AG22 sequence was used to study the structural induction and structural transition of G-quadruplexes by CD titration assays in the presence of the three compounds. As reported previously, the AG22 sequence is considered to show a summation spectrum involving multiple G-quadruplexes (mixed-type/basket-type) in K^+ solution from NMR data obtained for AG22[51]. The sequences Tel26 and wild-type Tel26 which both contain the AG22 four-G-tract human telomeric core sequence and have been well-defined based on NMR and CD data obtained with mixed-type G-quadruplexes, exhibit a distinct CD spectrum including a strong positive peak around 295 nm, with a shoulder peak around 268 nm and a smaller negative peak at 240 nm[50–52]. When different concentrations of the compounds were added to the K^+ solution of AG22, very similar CD spectra (Fig. 3) were generated to the Tel26 and wild-type Tel26 which had been confirmed the mixed-type G-quadruplex conformation, demonstrating that the compounds may induce the formation of mixed-type G-quadruplex. In the absence of any metal cations, the CD spectra consist of a positive band at 257 nm, a small positive band at 295 nm and a small negative peak near 240 nm, as shown in Figure 3. When the concentrations of the compounds were increased, there was an obvious decrease observed at 257 nm, accompanied by a sharp increase around 295 nm. These data suggest that all of the compounds, especially the two Pt(II) complexes, probably induced the conformation of a mixed-type parallel/antiparallel G-quadruplex structure and stabilized this structure[38,53]. These CD phenomena were consistent with the findings of Zhou *et al.*[54]. Similar conclusions were drawn based on a more identifiable conformation transition detected using 100 mM Na^+, and parallel experiments also roughly demonstrated the selectivity of the compounds towards the mixed-type stranded topology.

Inhibition of telomerase activity. To obtain further information about whether the compounds could inhibit telomerase activity and affect telomere elongation by telomerase, we performed the telomeric repeat amplification protocol (TRAP) assays, which can qualitatively and quantitatively evaluate the inhibition of telomerase[9,42,55–57]. In these assays, the elongated telomeres were further amplified by PCR cycling and could be visualized with dye staining. From the results presented in Figure 4, it is clear that the three compounds inhibited telomere elongation in a concentration-dependent manner, while the amplification of the internal telomerase assay standard (ITAS) control was not obviously affected. Thus, it was the telomerase activity rather than the PCR procedure itself that was inhibited by the three compounds. The inhibition of telomerase by the two complexes was found to be due to their function as strong G-quadruplex binders, showing IC_{50} values of 0.113 ± 0.019 and 3.69 ± 0.53 μM, respectively. Thus, complexes **1** and **2** exhibited stronger telomerase inhibition than dptmp (IC_{50} = 12.3 ± 1.2 μM).

Discussion

Guanine-rich sequences, which can form high-order G-quadruplex secondary structures, have been reported to be widely distributed in the human genome. Because of the potentially significant role of G-quadruplexes in the development of anticancer drugs, further research has been conducted on these compounds, for example, addressing G-quadruplex binders and telomerase inhibitors. In our studies, the interactions between the three compounds and hTel G-quadruplex sequences were investigated using FRET, SPR, CD and PCR stop assays. From the obtained FRET data, we conclude that the ΔT_m values of the two V-shaped dinuclear Pt(II) complexes were much higher than those previously reported for a modified phenanthroline-platinum(II) complex (20°C at 1.0 μM, FRET)[24] and [Pt(dppz-COOH)(N-C)]CF_3SO_3 (14°C at 20 μM, UV melting study)[58] and similar to those of tetranuclear platinum(II) complexes (34.5°C at 0.75 μM, 33.5°C and 32.1°C at 0.5 μM, FRET)[27,28]. Thus, the three compounds exhibited specific recognition abilities for different sequences of hTel G-quadruplex DNA. Furthermore, the obtained extremely low ΔT_m values demonstrate their poor stabilities with promoter sequences (c-myc and bcl2) and duplex DNA. The results obtained from SPR studies demonstrate the selectivity differences of the three compounds, with dptmp displaying little impact on G-qudruplex interaction, while **2** had a moderate selectivity and **1**

Table 2 | Kinetic parameters determined with SPR spectroscopy[a,b,c]

	dptmp		**1**		**2**	
	hTel	duplex	hTel	duplex	hTel	duplex
k_a (M^{-1} s^{-1})[a]	1.40×10^4	1.56×10^4	1.12×10^5	1.83×10^5	1.27×10^5	3.60×10^4
k_d (s^{-1})[a]	3.51×10^{-2}	4.50×10^{-2}	8.22×10^{-2}	9.48×10^{-1}	9.01×10^{-2}	1.22×10^{-1}
K_D (M)[b]	2.50×10^{-6}	2.89×10^{-6}	7.31×10^{-7}	5.17×10^{-6}	7.12×10^{-7}	3.39×10^{-6}
K_A (M^{-1})[b]	4.00×10^5	3.46×10^5	1.37×10^6	1.93×10^5	1.40×10^6	2.95×10^5
Chi2 (RU)[c]	6.68	9.42	5.09	2.55	10.69	15.55

[a]k_a is the association rate constant, while k_d is the dissociation rate constant.
[b]K_D was calculated through global fitting of the kinetic data obtained for various concentrations of the compounds using a two-state binding model; K_D is given by k_d/k_a, and K_A was determined from k_a/k_d.
[c]The Chi2 value is a statistical measure of the closeness of the fit. Chi2 was of the same order of magnitude as the noise in RU. The fitting process was terminated automatically when a minimum value was found for Chi2.

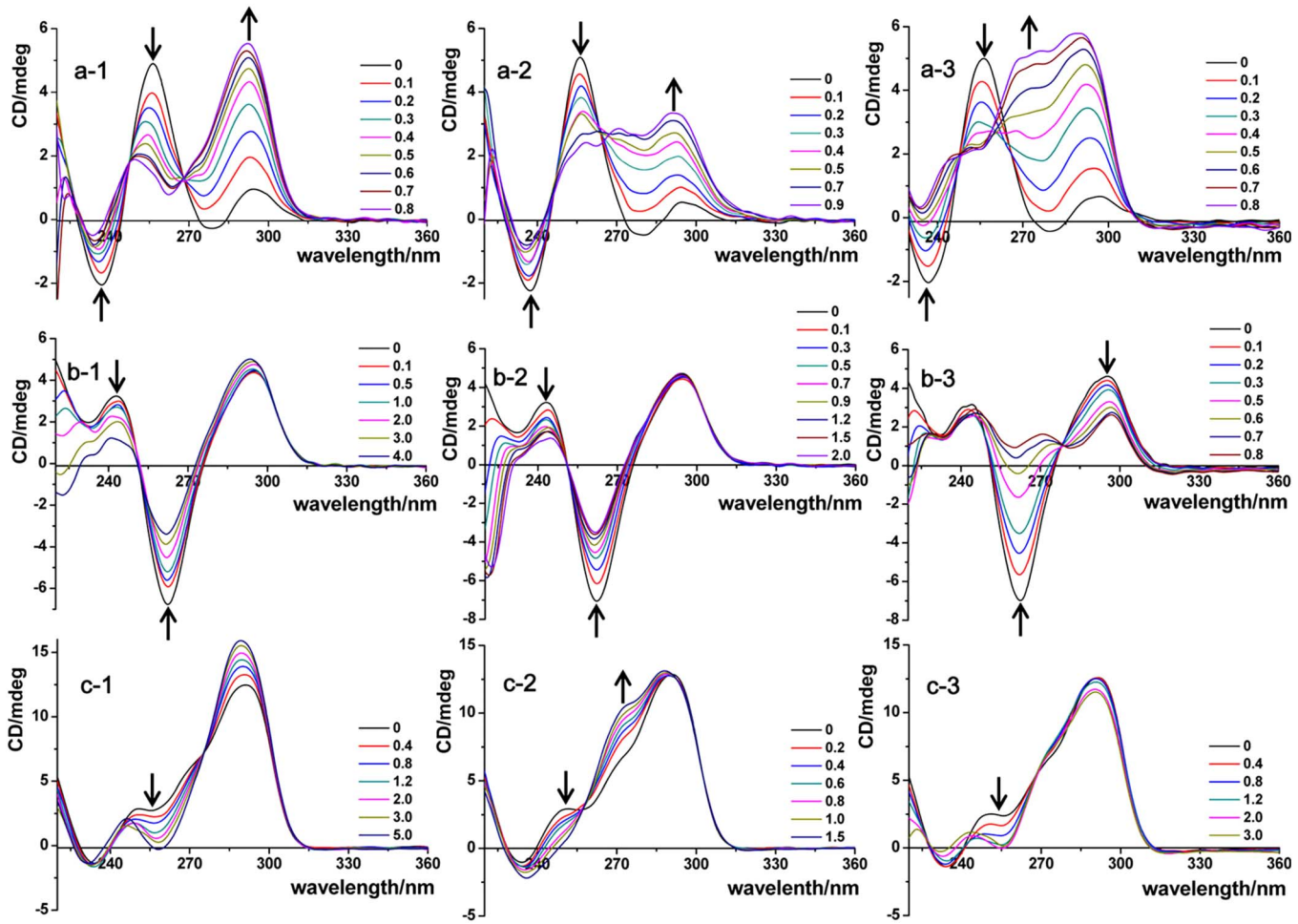

Figure 3 | **CD titration spectra of the human telomeric G-quadruplexes (3.0 μM) induced by the three compounds (from left to right: dptmp, 1 and 2) in 10 mM Tris-HCl, pH 7.4, at room temperature ($r = C_{ML}/C_{DNA}$).** a: In the absence of metal ions; b: In 100 mM NaCl; c: In 100 mM KCl.

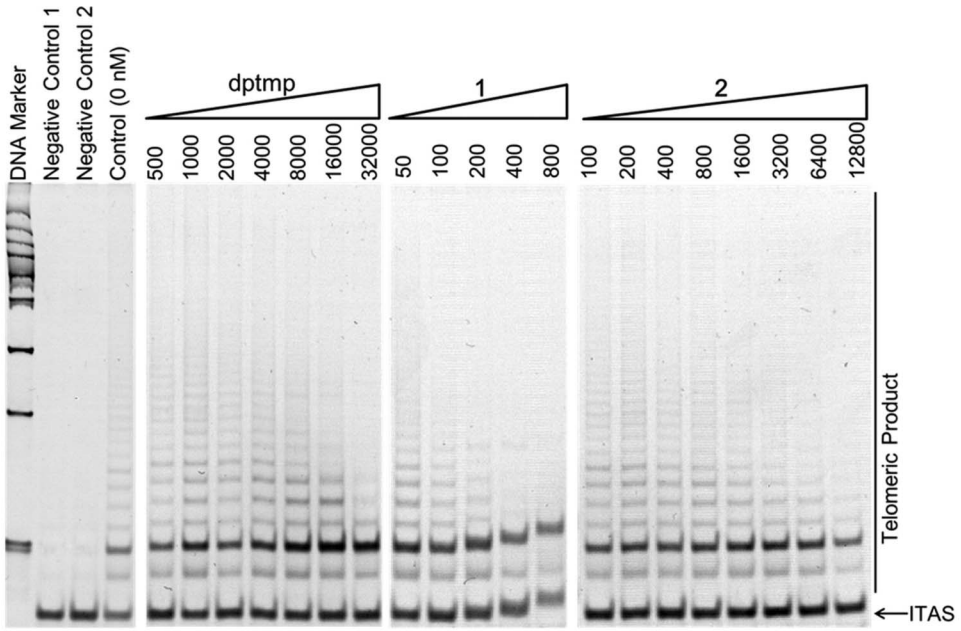

Figure 4 | **TRAP assay[a] results for the three compounds (dptmp, 1 and 2), showing telomeric ladders produced by PCR amplification of the oligonucleotides generated by the action of telomerase on a TS primer. The lower band is an internal control primer (ITAS).** [a] Each single assay was dependent on 1.0 μL of telomerase extract (200 cells), prepared from HeLa cells with NP-40 lysis buffer. Negative controls 1 and 2, which accompanied every assay, involved either incubating approximately 1.0 μL of cell lysate at 85°C for 10 min before primer extension or incubating approximately 1.0 μL of NP-40 lysis buffer, respectively. The control (0 nM) assay was performed without adding any compound.

had the highest selectivity. Furthermore, both Pt(II) complexes show preferential quadruplex/duplex DNA selectivity compared to corresponding dptmp, highlighting the importance of the platinum(II) moiety in defining their binding ability. This might be attributed to the platinum(II) moiety that can interact with both the grooves and loops of the hTel quadruplex and their negatively charged phosphate backbones.

The data obtained from PCR stop assays were consistent with previous results, demonstrating that both Pt(II) complexes **1** and **2**, especially **1**, exhibited an excellent stability towards hTel G-quadruplex, binding more effectively than the corresponding ligand-dptmp. We were able to obtain the exact conformation of the mixed-type stranded topology induced by the three compounds from the CD assays. Another result that should be paid attention to is that the two Pt(II) complexes were considered to show reasonable inhibition of telomerase activity based on the TRAP studies.

In conclusion, we have prepared a water-soluble, quaternized trigeminal ligand and its two derivative Pt(II) complexes. X-ray diffraction analysis showed that the dinuclear Pt(II) complex exhibited a V-shaped structure. Further biochemical assays confirmed that the ligand and the two complexes, especially complex **1**, coordinated by straight-chain polyamine, can selectively stabilize the human telomeric G-quadruplex, likely induce the formation of mixed-type parallel/antiparallel G-quadruplex structure and significantly inhibit the activity of telomerase, probably due to interactions with the sugar-phosphate backbone of the G-quadruplex. Thus, the Pt(II) complexes exhibit a potential promise for antitumor therapies and need to be further investigated to clarify their specific biochemical details.

Methods

Materials. All chemicals and solvents were obtained from commercial sources and used without further purification.

Synthesis of 4-[4,6-di(4-pyridyl)-1,3,5-(2-triazinyl)]-1-methylpyridine-1-ium iodide $C_{19}H_{15}N_6{\cdot}I$ (dptmp·I): A mixture of tpt (0.62 g, 2.00 mmol) and MeI (0.85 g, 6.00 mmol) in trichloromethane (240 mL) was stirred at 61°C for 48 h in darkness. The solution gradually became red and a red precipitate formed. The resulting slurry was collected by filtration, and the residue was washed with trichloromethane (2 × 10 mL) to remove tpt. The obtained product was dried under vacuum to give a red powder (yield: 0.79 g, 86%). Yellow crystals were grown from an aqueous solution standing in air at room temperature and characterized by X-ray structure analysis. ^{1}H NMR (Supplementary Fig. S2) (300 MHz, D_2O): δ 8.92 (d, J = 6.3 Hz, 2H), 8.72 (d, J = 6.0 Hz, 2H), 8.40 (d, J = 4.8 Hz, 4H), 8.00 (d, J = 4.8 Hz, 4H), 4.538 (s, 3H); ^{13}C NMR (Supplementary Fig. S3) (75 MHz, $(CD_3)_2SO$): δ 171.8, 168.7, 151.5, 149.7, 147.6, 142.5, 126.9, 123.1, 49.0. ESI-MS (Supplementary Fig. S1) (H_2O) anal. calcd. for $C_{19}H_{15}N_6$, $[L\text{-}I^-]^+$ (m/z) 327.4, found 327.36. Elemental analysis (anal. calcd., found for $C_{19}H_{15}N_6I{\cdot}1.5H_2O$): C (47.41, 47.72), H (3.77, 3.97), N (17.46, 17.44).

Synthesis of 4-[4,6-di(4-pyridyl)-1,3,5-(2-triazinyl)]-1-methylpyridine-1-ium hexafluorophosphate $C_{19}H_{15}N_6{\cdot}PF_6$ (dptmp·PF_6): The red powder of dptmp·I (0.16 g, 0.35 mmol) was dissolved in a sufficient amount of water, and ammonium hexafluorophosphate (0.50 g, 3.06 mmol) was then added to the solution, and a pale solid precipitated immediately. The product was filtered, washed from the filter twice with 2 × 10 mL ethanol and then dried under vacuum (0.17 g, quantitative yield). Elemental analysis (anal. calcd., found for $C_{19}H_{15}N_6PF_6$): C (48.31, 48.23), H (3.20, 3.45), N (17.79, 17.76).

Synthesis of $\{[Pt(dien)]_2(dptmp)\}(PF_6)_5$ (**1**): [Pt(dien)Cl]Cl·HCl was synthesized through a method similar to that described by Giuliano Annibale[34], using $[Pt(COD)Cl_2]$[35] as an intermediate. $[Pt(COD)Cl_2]$ (0.25 g, 0.67 mmol) in methyl alcohol (about 50 mL), diethylenetriamine (68.9 mg, 0.67 mmol) was added with stirring and the mixture was heated at 40–50°C. After 15 min, the solid dissolved, and a clear, pale yellow solution was obtained, which was cooled to room temperature and then filtered to remove any unreacted COD complex. Water was then removed under reduced pressure, leaving a pale yellow solid, which was collected and washed thoroughly with diethyl ether and then air dried (yield: 0.24 g, 96.7%). [Pt(dien)Cl]Cl·HCl (87 mg, 0.22 mmol) and $AgNO_3$ (0.11 g, 0.65 mmol) in water (9 mL) were stirred in a stoppered flask in darkness for 48 h at 45°C and then filtered to remove AgCl. The clear filtrate was subsequently transferred to another stoppered flask, to which dptmp·PF_6 (47 mg, 0.10 mmol) was added, followed by heating at 90°C for 72 h under N_2. The whole experiment was conducted in darkness. The resulting solution was collected by filtration, after which excess ammonium hexafluorophosphate was added to the filtrate, and a white product precipitated immediately. Finally, the resulting slurry was filtered, and the product washed twice from the filter with 2 × 10 mL of ethanol, then dried under vacuum (0.13 g, 72%). Pale crystals were grown from an acetonitrile-water (1:5) mixture standing in air at room temperature and characterized by X-ray structure analysis (Fig. 1 and Table S1, S2). ^{1}H NMR (Supplementary Fig. S4) (300 MHz, $(CD_3)_2SO$): δ 9.39 (d, J = 6.0 Hz, 2H), 9.30 (d, J = 6.0 Hz, 2H), 9.09 (d, J = 6.0 Hz, 4H), 8.98 (d, J = 6.0 Hz, 4H), 7.45 (broad, 2H), 6.16 (d, J = 6.0 Hz, 4H), 6.03 (d, J = 6.0 Hz, 4H), 4.52 (s, 3H), 3.17–2.77 (m, 16H); ^{13}C NMR (Supplementary Fig. S5) (100 MHz, $(CD_3)_2SO$): δ 170.2, 168.9, 154.2, 149.1, 147.1, 144.8, 126.9, 126.0, 54.6, 50.3, 48.9; ^{195}Pt NMR (^{1}H 400 MHz, $(CD_3)_2SO$): −1,196.23 ppm, and K_2PtCl_4 was used as an internal reference (δ = 0). Elemental analysis (anal. calcd., found for $\{[Pt(dien)]_2(dptmp)\}(PF_6)_5$): C (19.67, 19.43), H (2.51, 2.76), N (10.19, 10.11).

$\{[Pt(dpa)]_2(dptmp)\}(PF_6)_5$ (**2**) was synthesized with a high yield of 95.3% as above synthesis method of **1**, except that the first procedure of treating with $AgNO_3$ should be 60°C for 40 h. The complex of $[Pt(dpa)Cl]Cl.2H_2O$ was synthesized according to a procedure described in the literature[59]. ^{1}H NMR (Supplementary Fig. S6) (300 MHz, $(CD_3)_2SO$): δ 9.47–8.75 (m, 12H), 8.29 (t, J = 6.0 Hz, 4H), 7.89 (d, J = 6.0 Hz, 4H), 7.73 (t, J = 6.0 Hz, 4H), 7.49 (t, J = 6.0 Hz, 4H), 5.01–4.52 (m, 11H); ^{13}C NMR (Supplementary Fig. S7) (100 MHz, $(CD_3)_2SO$): δ 172.1, 170.5, 169.9, 169.2, 168.9, 167.0, 154.6, 151.7, 149.1, 147.6, 145.6, 142.3, 127.6, 126.8, 126.1, 123.9, 122.9, 59.4, 48.9. ^{195}Pt NMR (^{1}H 400 MHz, $(CD_3)_2SO$): −770.2 ppm, and K_2PtCl_4 was used as an internal reference (δ = 0). Elemental analysis (anal. calcd., found for $\{[Pt(dpa)]_2(dptmp)\}(PF_6)_5{\cdot}CH_3CN$): C (28.72, 28.85), H (2.36, 2.52), N (9.68, 9.46).

X-ray diffraction measurements. The intensity data were recorded using an Agilent Xcalubur Nova CCD diffractometer with graphite monochromated Cu Kα radiation (**1**, λ = 1.54178 Å) at 293(2) K, a Rigaku R-AXIS SPIDE IP system with Mo Kα radiation (dptmp, λ = 0.71073 Å) at 298(2) K and a Brucker Smart 1000 CCD diffractometer with Mo Kα radiation ($[Pt(dpa)NO_3]PF_6$, λ = 0.71073 Å) at 173(2) K. The structures of dptmp, **1** and $[Pt(dpa)NO_3]PF_6$ (CCDC 904100) were solved via direct methods and refined using a full-matrix least-squares technique with SHELXTL program package. All non-hydrogen atoms were refined using anisotropic displacement parameters. All hydrogen atoms on organic ligands were generated in riding mode. The obtained crystallographic data and the details of the refinement of dptmp, **1** and $[Pt(dpa)NO_3]PF_6$ are listed in Supplementary Table S1 and the bond lengths and bond angles are given in Supplementary Tables S2–S4.

Fluorescence resonance energy transfer (FRET) studies. The employed FRET probes included a fluorescently labeled hTel oligonucleotide (5′-FAM-[GGGTTAGGGTTAGGGTTAGGG]-TAMRA-3′, mimicking the human telomeric repeat, FAM: 6-carboxyfluorescein, TAMRA: 6-carboxytetramethylrhodamine, Sangon), three promoter sequences (c-myc: 5′-FAM-[TG4AGGGTGGGGAGGGTGGGGAAGG]-TAMRA-3′; bcl2: 5′-FAM-[AGGGGCGGGCGCGGGAGGAAGGGGGCGGGAGCGGGGCTG]-TAMRA-3′, Sangon) and a duplex DNA sequence (5′-FAM-[TATAGCTATA-HEG-TATAGCTATA]-TAMRA-3′, HEG linker: $[(-CH_2-CH_2-O-)_6]$, Sangon). The experiment procedure was as previously reported method[29]. Final analysis of the data was carried out using Origin 8.0 (OriginLab Corp.).

Surface plasmon resonance (SPR) studies. SPR measurements were conducted in a ProteOn XPR36 Protein Interaction Array system (Bio-Rad Laboratories, Hercules, CA, USA) using a Neutravidin-coated GLM sensor chip. Biosensor experiments[28,29] were conducted in filtered and degassed running buffer (Tris-HCl 50 mM pH 7.4, 300 mM KCl, 0.005% Tween-20) at 25°C. The biotinylated oligonucleotides used in these assays were Biotin-hTel (Quadruplex: 5′-biotin-[AGGGTTAGGGTTAGGGTTAGGG]-3′) and Biotin-duplex (5′-biotin-[CGAATTCGTCTCCGAATTCG]-3′). DNA samples were captured (approximately 1,200 RU) in flow cells dptmp, **1** and **2**, leaving the fourth flow cell as a blank. Data were analyzed with ProteOn manager software, using the two states model for fitting kinetic data.

Polymerase chain reaction (PCR) stop assays. The oligonucleotide sequence (HTG21, 5′-[GGGTTAGGGTTAGGGTTAGGG]-3′, Sangon) and the corresponding complementary sequence (HTG21rev, 5′-[ATCGCTTCTCGTCCC TAACC]-3′, Sangon) were used in this assay. The experiment procedure was as previously reported method[29,31]. A parallel experiment was performed using a mutated oligomer, HTG21mu (5′-[GAGTTAGAGTTAGAGTTAGAG]-3′, Sangon) with its corresponding complementary sequence HTG21murev (5′-[ATCGCTTCT CGTCTCTAACT]-3′, Sangon) instead of HTG21 and HTG21rev under the same conditions.

Circular dichroism (CD) measurements. CD spectra were measured using a J-810 spectropolarimeter (JASCO, Japan) with a 1 cm cell length quartz cell, over a wavelength range of 220-360 nm at a scan speed of 200 nm/min with five acquisitions at room temperature. The AG22 oligomer (5′-[AGGGTTAGGGTTA GGGTTAGGG]-3′, Sangon) was resuspended in Tris-HCl buffer (10 mM, pH 7.4) containing 100 mM K^+, 100 mM Na^+ or no metal cations. The experiment procedure was as previously reported method[29,31] and final analysis of the data was carried out using Origin 8.0 (OriginLab Corp.).

Telomeric repeat amplification protocol (TRAP) assays. A telomerase extract (1.0 μL, 200 cells) was prepared from HeLa cells with NP-40 lysis buffer (10 mM Tris-HCl, pH 8.0, 1.0 mM $MgCl_2$, 1.0 mM EGTA, 1.0% NP-40, 0.25 mM sodium deoxycholate, 10% glycerol, 150 mM NaCl, 5.0 mM beta-mercaptoethanol (β-ME), 0.1 mM PMSF). Each reaction was performed in a final volume of 20 μL in a reaction mixture containing of 2.0 μL of 10× TRAP buffer (200 mM Tris-HCl, pH 8.3,

15 mM $MgCl_2$, 630 mM KCl, 0.5% Tween-20 and 10 mM EGTA in DEPC-treated water), 1.6 μL of dNTP mix (2.5 mM, TaKaRa), 0.4 μL of TS primer (100 ng/μL, 5′-[AATCCGTCGAGCAGAGTT]-3′, Invitrogen), 0.8 μL Primer mix (ACX reverse primer, 100 ng/μL, 5′-[GCGCGGCTTACCCTTACCCTTACCCTAACC]-3′ and NT primer 100 ng/μL, 5′-[ATCGCTTCTCGGCCTTTT]-3′, Invitrogen), 2.0 μL TSNT internal control primer (4.0×10^{-11} M, 5′-[AATCCGTCGAGCAGAGTTAA AAGGCCGAGAAGCGAT]-3′, Invitrogen), 0.4 μL of RNase inhibitor (2 U/μL, TaKaRa), 0.16 μL of Taq polymerase (5 U/μL, TaKaRa), 5.0 μL of different concentrations of the compounds and 6.64 μL of DEPC-treated water. Two negative controls (designated 1 and 2) accompanied with each assay: negative control 1 involved incubating approximately 1.0 μL of cell lysate at 85°C for 10 min prior to primer extension, while negative control 2 was also included involved the incubation of approximately 1.0 μL of NP-40 lysis buffer. The experiment procedure was as previously reported method[28,29].

1. Gellert, M., Lipsett, M. N. & Davies, D. R. Helix formation by guanylic acid. *Proc. Natl. Acad. Sci. U. S. A.* **48**, 2013–2018 (1962).
2. Patel, D. J., Phan, A. T. & Kuryavyi, V. Human telomere, oncogenic promoter and 5'-UTR G-quadruplexes: diverse higher order DNA and RNA targets for cancer therapeutics. *Nucleic Acids Res.* **35**, 7429–7455 (2007).
3. Hou, J. Q. *et al*. Impact of planarity of unfused aromatic molecules on G-quadruplex binding: learning from isaindigotone derivatives. *Org. Biomol. Chem.* **9**, 6422–6436 (2011).
4. Huppert, J. L. & Balasubramanian, S. G-quadruplexes in promoters throughout the human genome. *Nucleic Acids Res.* **35**, 406–413 (2007).
5. Todd, A. K. Bioinformatics approaches to quadruplex sequence location. *Methods* **43**, 246–251 (2007).
6. Todd, A. K., Haider, S. M., Parkinson, G. N. & Neidle, S. Sequence occurrence and structural uniqueness of a G-quadruplex in the human c-kit promoter. *Nucleic Acids Res.* **35**, 5799–5808 (2007).
7. Kim, N. W. *et al*. Specific association of human telomerase activity with immortal cells and cancer. *Science* **266**, 2011–2015 (1994).
8. Counter, C. M., Hirte, H. W., Bacchetti, S. & Harley, C. B. Telomerase activity in human ovarian carcinoma. *Proc. Natl. Acad. Sci. U. S. A.* **91**, 2900–2904 (1994).
9. Zahler, A. M., Williamson, J. R., Cech, T. R. & Prescott, D. M. Inhibition of telomerase by G-quartet DNA structures. *Nature* **350**, 718–720 (1991).
10. Parkinson, G. N., Lee, M. P. & Neidle, S. Crystal structure of parallel quadruplexes from human telomeric DNA. *Nature* **417**, 876–880 (2002).
11. Lim, K. W. *et al*. Coexistence of two distinct G-quadruplex conformations in the hTERT promoter. *J. Am. Chem. Soc.* **132**, 12331–12342 (2010).
12. Wang, Y. & Patel, D. J. Solution structure of the human telomeric repeat $d[AG_3(T_2AG_3)_3]$ G-tetraplex. *Structure* **1**, 263–282 (1993).
13. Wang, P., Leung, C. H., Ma, D. L., Yan, S. C. & Che, C. M. Structure-based design of platinum(II) complexes as c-myc oncogene down-regulators and luminescent probes for G-quadruplex DNA. *Chem. Eur. J.* **16**, 6900–6911 (2010).
14. Read, M. *et al*. Structure-based design of selective and potent G quadruplex-mediated telomerase inhibitors. *Proc. Natl. Acad. Sci. U. S. A.* **98**, 4844–4849 (2001).
15. Shin-ya, K. *et al*. Telomestatin, a novel telomerase inhibitor from Streptomyces anulatus. *J. Am. Chem. Soc.* **123**, 1262–1263 (2001).
16. Shi, D. F., Wheelhouse, R. T., Sun, D. & Hurley, L. H. Quadruplex-interactive agents as telomerase inhibitors: synthesis of porphyrins and structure-activity relationship for the inhibition of telomerase. *J. Med. Chem.* **44**, 4509–4523 (2001).
17. Harrison, R. J. *et al*. Trisubstituted acridine derivatives as potent and selective telomerase inhibitors. *J. Med. Chem.* **46**, 4463–4476 (2003).
18. Gunaratnam, M. *et al*. G-quadruplex compounds and cis-platin act synergistically to inhibit cancer cell growth in vitro and in vivo. *Biochem. Pharmacol.* **78**, 115–122 (2009).
19. Drygin, D. *et al*. Anticancer activity of CX-3543: a direct inhibitor of rRNA biogenesis. *Cancer Res.* **69**, 7653–7661 (2009).
20. Gowan, S. M., Heald, R., Stevens, M. F. & Kelland, L. R. Potent inhibition of telomerase by small-molecule pentacyclic acridines capable of interacting with G-quadruplexes. *Mol. Pharmacol.* **60**, 981–988 (2001).
21. Reed, J. E., Arnal, A. A., Neidle, S. & Vilar, R. Stabilization of G-quadruplex DNA and inhibition of telomerase activity by square-planar nickel(II) complexes. *J. Am. Chem. Soc.* **128**, 5992–5993 (2006).
22. Dixon, I. M. *et al*. A G-quadruplex ligand with 10000-fold selectivity over duplex DNA. *J. Am. Chem. Soc.* **129**, 1502–1503 (2007).
23. Bianco, S. *et al*. Bis-phenanthroline derivatives as suitable scaffolds for effective G-quadruplex recognition. *Dalton Trans.* **39**, 5833–5841 (2010).
24. Reed, J. E., Neidle, S. & Vilar, R. Stabilisation of human telomeric quadruplex DNA and inhibition of telomerase by a platinum-phenanthroline complex. *Chem. Commun.* 4366–4368 (2007).
25. Reed, J. E., White, A. J., Neidle, S. & Vilar, R. Effect of metal coordination on the interaction of substituted phenanthroline and pyridine ligands with quadruplex DNA. *Dalton Trans.* 2558–2568 (2009).
26. Suntharalingam, K., White, A. J. & Vilar, R. Synthesis, structural characterization, and quadruplex DNA binding studies of platinum(II)-terpyridine complexes. *Inorg. Chem.* **48**, 9427–9435 (2009).
27. Kieltyka, R. *et al*. A platinum supramolecular square as an effective G-quadruplex binder and telomerase inhibitor. *J. Am. Chem. Soc.* **130**, 10040–10041 (2008).
28. Zheng, X. H., Chen, H. Y., Tong, M. L., Ji, L. N. & Mao, Z. W. Platinum squares with high selectivity and affinity for human telomeric G-quadruplexes. *Chem. Commun.* **48**, 7607–7609 (2012).
29. Zheng, X. H., Zhong, Y. F., Tan, C. P., Ji, L. N. & Mao, Z. W. Pt(II) squares as selective and effective human telomeric G-quadruplex binders and potential cancer therapeutics. *Dalton Trans.* **41**, 11807–11812 (2012).
30. Suntharalingam, K., White, A. J. & Vilar, R. Two metals are better than one: investigations on the interactions between dinuclear metal complexes and quadruplex DNA. *Inorg. Chem.* **49**, 8371–8380 (2010).
31. Wang, J. T. *et al*. 1,10-Phenanthroline platinum(II) complex: a simple molecule for efficient G-quadruplex stabilization. *Dalton Trans.* **39**, 7214–7216 (2010).
32. Wang, J. T., Li, Y., Tan, J. H., Ji, L. N. & Mao, Z. W. Platinum(II)-triarylpyridines complexes with electropositive pendants as efficient G-quadruplex binders. *Dalton Trans.* **40**, 564–566 (2011).
33. Weber, C. F. & van Eldik, R. Influence of solvent on ligand-substitution reactions of Pt-II complexes as function of the pi-acceptor properties of the spectator chelate. *Eur. J. Inorg. Chem.* 4755–4761 (2005).
34. Annibale, G., Brandolisio, M. & Pitteri, B. New routes for the synthesis of chloro(diethylenetriamine) platinum(II) chloride and chloro(2,2′ : 6′,2″-terpyridine) platinum(II) chloride dihydrate. *Polyhedron* **14**, 451–453 (1995).
35. McDermott, J. X., White, J. F. & Whitesides, G. M. Thermal decomposition of bis(phosphine)platinum(II) metallocycles. *J. Am. Chem. Soc.* **98**, 6521–6528 (1976).
36. Mergny, J.-L. & Maurizot, J.-C. Fluorescence Resonance Energy Transfer as a Probe for G-Quartet Formation by a Telomeric Repeat. *ChemBioChem* **2**, 124–132 (2001).
37. Rezler, E. M. *et al*. Telomestatin and Diseleno Sapphyrin Bind Selectively to Two Different Forms of the Human Telomeric G-Quadruplex Structure. *J. Am. Chem. Soc.* **127**, 9439–9447 (2005).
38. Ren, L. *et al*. Quaternary ammonium zinc phthalocyanine: inhibiting telomerase by stabilizing G quadruplexes and inducing G-quadruplex structure transition and formation. *ChemBioChem* **8**, 775–780 (2007).
39. Han, H., Hurley, L. H. & Salazar, M. A DNA polymerase stop assay for G-quadruplex-interactive compounds. *Nucleic Acids Res.* **27**, 537–542 (1999).
40. Lemarteleur, T. *et al*. Stabilization of the c-myc gene promoter quadruplex by specific ligands' inhibitors of telomerase. *Biochem. Biophys. Res. Commun.* **323**, 802–808 (2004).
41. Balagurumoorthy, P. & Brahmachari, S. K. Structure and stability of human telomeric sequence. *J. Biol. Chem.* **269**, 21858–21869 (1994).
42. Teulade-Fichou, M. P. *et al*. Selective recognition of G-qQuadruplex telomeric DNA by a bis(quinacridine) macrocycle. *J. Am. Chem. Soc.* **125**, 4732–4740 (2003).
43. Bugaut, A. *et al*. Exploring the differential recognition of DNA G-quadruplex targets by small molecules using dynamic combinatorial chemistry. *Angew. Chem. Int. Ed.* **47**, 2677–2680 (2008).
44. Rodriguez, R., Pantoş, G. D., Gonçalves, D. P. N., Sanders, J. K. M. & Balasubramanian, S. Ligand-Driven G-Quadruplex Conformational Switching By Using an Unusual Mode of Interaction. *Angew. Chem. Int. Ed.* **119**, 5501–5503 (2007).
45. Jaumot, J. & Gargallo, R. Experimental methods for studying the interactions between G-quadruplex structures and ligands. *Curr. Pharm. Design* **18**, 1900–1916 (2012).
46. Li, W., Wu, P., Ohmichi, T. & Sugimoto, N. Characterization and thermodynamic properties of quadruplex/duplex competition. *FEBS Lett.* **526**, 77–81 (2002).
47. Zhou, J. L. *et al*. Synthesis and evaluation of quindoline derivatives as G-quadruplex inducing and stabilizing ligands and potential inhibitors of telomerase. *J. Med. Chem.* **48**, 7315–7321 (2005).
48. Goncalves, D. P., Rodriguez, R., Balasubramanian, S. & Sanders, J. K. Tetramethylpyridiniumporphyrazines--a new class of G-quadruplex inducing and stabilising ligands. *Chem. Commun.* 4685–4687 (2006).
49. Giraldo, R., Suzuki, M., Chapman, L. & Rhodes, D. Promotion of parallel DNA quadruplexes by a yeast telomere binding protein: a circular dichroism study. *Proc. Natl. Acad. Sci. U. S. A.* **91**, 7658–7662 (1994).
50. Dai, J., Carver, M., Punchihewa, C., Jones, R. A. & Yang, D. Structure of the Hybrid-2 type intramolecular human telomeric G-quadruplex in K+ solution: insights into structure polymorphism of the human telomeric sequence. *Nucleic Acids Res.* **35**, 4927–4940 (2007).
51. Ambrus, A. *et al*. Human telomeric sequence forms a hybrid-type intramolecular G-quadruplex structure with mixed parallel/antiparallel strands in potassium solution. *Nucleic Acids Res.* **34**, 2723–2735 (2006).
52. Dai, J. *et al*. Structure of the intramolecular human telomeric G-quadruplex in potassium solution: a novel adenine triple formation. *Nucleic Acids Res.* **35**, 2440–2450 (2007).
53. Fu, B. *et al*. Cationic corrole derivatives: a new family of G-quadruplex inducing and stabilizing ligands. *Chem. Commun.* 3264–3266 (2007).
54. Fu, B. *et al*. Cationic metal-corrole complexes: design, synthesis, and properties of guanine-quadruplex stabilizers. *Chem. Eur. J.* **14**, 9431–9441 (2008).
55. Riou, J. F. *et al*. Cell senescence and telomere shortening induced by a new series of specific G-quadruplex DNA ligands. *Proc. Natl. Acad. Sci. U. S. A.* **99**, 2672–2677 (2002).
56. Anantha, N. V., Azam, M. & Sheardy, R. D. Porphyrin binding to quadrupled T4G4. *Biochemistry* **37**, 2709–2714 (1998).

57. Wheelhouse, R. T., Sun, D., Han, H., Han, F. X. & Hurley, L. H. Cationic Porphyrins as Telomerase Inhibitors: the Interaction of Tetra-(N-methyl-4-pyridyl)porphine with Quadruplex DNA. *J. Am. Chem. Soc.* **120**, 3261–3262 (1998).
58. Ma, D.-L., Che, C.-M. & Yan, S.-C. Platinum(II) Complexes with Dipyridophenazine Ligands as Human Telomerase Inhibitors and Luminescent Probes for G-Quadruplex DNA. *J. Am. Chem. Soc.* **131**, 1835–1846 (2008).
59. Correia, I. & Welton, T. An old reaction in new media: kinetic study of a platinum(II) substitution reaction in ionic liquids. *Dalton Trans.* 4115–4121 (2009).

Acknowledgments

The authors thank Prof. Rudi van Eldik for the valuable help. This work was supported by the National Natural Science Foundation of China (Nos., 21172274, 21121061, 21231007 and J1103305), the Guangdong Provincial Natural Science Foundation (No. 9351027501000003), the Ministry of Education of China (Nos., 20100171110013 and 313058), the National High-Tech Research and Development Programme of China (863 Program, Grant 2012AA020305) and the Fundamental Research Funds for the Central Universities.

Author contributions

C.X.X. and Z.W.M. conceived and designed the experiments. C.X.X., Y.X.Z. and X.H.Z. conducted the synthetic experiments. Q.H. conducted the TRAP assays. Y.Z. helped C.X.X. in the TRAP data analysis. L.N.J. provided effective directions during the research process. C.X.X. and Z.W.M. wrote the manuscript. All authors discussed the results and commented on the manuscript. All authors reviewed the manuscript.

Additional information

Supplementary information accompanies this paper at http://www.nature.com/scientificreports

Competing financial interests: The authors declare no competing financial interests.

How to cite this article: Xu, C.-X. *et al.* V-Shaped Dinuclear Pt(II) Complexes: Selective Interaction with Human Telomeric G-quadruplex and Significant Inhibition towards Telomerase. *Sci. Rep.* **3**, 2060; DOI:10.1038/srep02060 (2013).